Shear and bulk viscosities of gluon plasma across the transition temperature from lattice QCD

Heng-Tong Ding [1] Hai-Tao Shu [1] **Cheng Zhang** [1]

[1]Central China Normal University, Wuhan, China

Nuclear Science Computing Center at CCNU

Viscosity of Gluon Plasma

- Experimental constraints of shear viscosity: $1/(4\pi) < \eta/s < 3/(4\pi)$ [1]:
- Bulk viscosity based on leading-order perturbative result: for $0.06 < \alpha_s < 0.3, \zeta/s \approx 0.02\alpha_s^2$ [2].
- Temperature dependence of viscosity using multilevel algorithm [3, 4].
- Temperature dependence of viscosity using gradient flow [5]: extendable to full QCD.

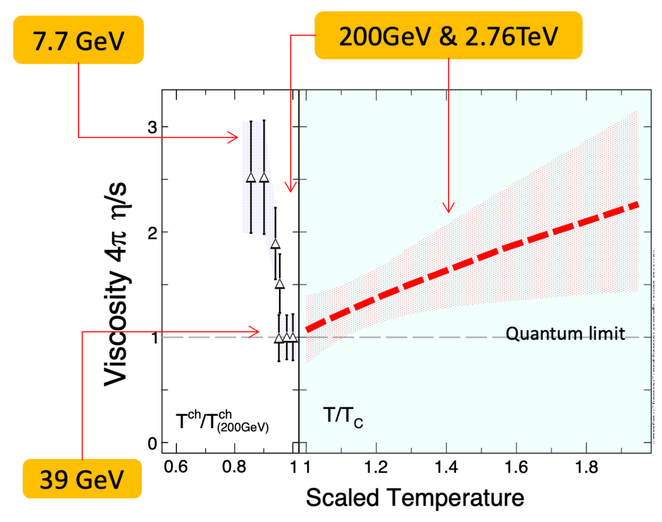

Courtesy of Nu Xu.

Theoretical Framework

1. The Euclidean energy-momentum tensor (EMT) correlators $\xrightarrow{\text{inverse}}$ spectral function.

$$G_{\text{shear}}(\tau) = \frac{1}{10}\int d^3x \langle \pi_{ij}(0,\vec{0})\pi_{ij}(\tau,\vec{x})\rangle, \quad G_{\text{bulk}}(\tau) = \int d^3x \Big\langle T_{\mu\mu}(0,\vec{0})T_{\mu\mu}(\tau,\vec{x})\Big\rangle.$$

$$G_{\text{shear/bulk}}(\tau) = \int_0^\infty \frac{dw}{\pi}\frac{\cosh[w(1/2T-\tau]}{\sinh(w/2T)}\rho_{\text{shear/bulk}}(w,T).$$

2. Spectral function $\xrightarrow{\text{Kubo formula}} \zeta, \eta$.

$$\eta(T) = \lim_{\omega\to 0}\frac{\rho_{shear}(\omega,T)}{\omega}, \quad \zeta(T) = \frac{1}{9}\lim_{\omega\to 0}\frac{\rho_{bulk}(\omega,T)}{\omega}.$$

3. Model spectral function:

$$\frac{\rho(\omega)}{\omega T^3} = \frac{A}{T^3}\frac{C^2}{C^2+(\omega/T)^2} + B\frac{\rho_{\text{pert}}(\omega)}{\omega T^3}, \ \frac{A}{T^3}\frac{C^2 m(\omega/T)}{C^2+(\omega/T)^2} + B\frac{\rho_{\text{pert}}(\omega)}{\omega T^3}\big(1-m(\omega/T)\big).$$

4. Noise reduction techniques:
   - Gradient flow:

$$\dot{B}_\mu = (\partial_\mu + [B_\mu,\cdot])(\partial_\mu B_\nu - \partial_\nu B_\mu + [B_\mu, B_\nu]).$$

LO solution:

$$B_\nu(x,\tau_F) = \int \mathrm{d}y \Big(\frac{\sqrt{2\pi(8\tau_F)}}{2}\Big)^{-4}\exp\Big(\frac{-(x-y)^2}{\sqrt{8\tau_F}^2/2}\Big)B_\nu(y).$$

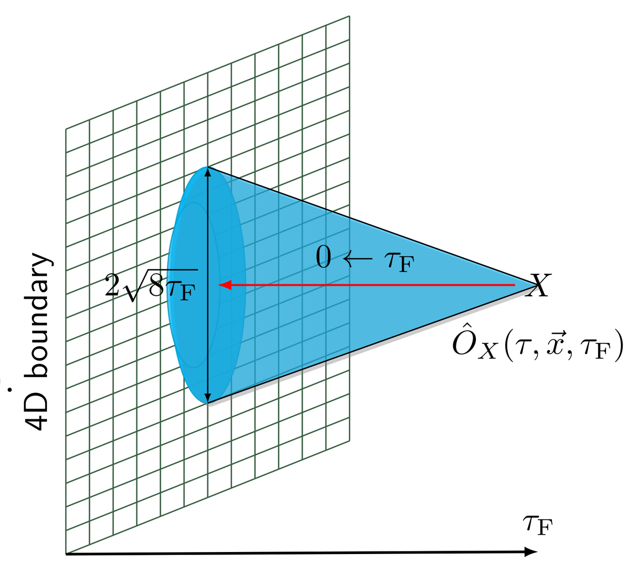

   - Blocking method [6]:

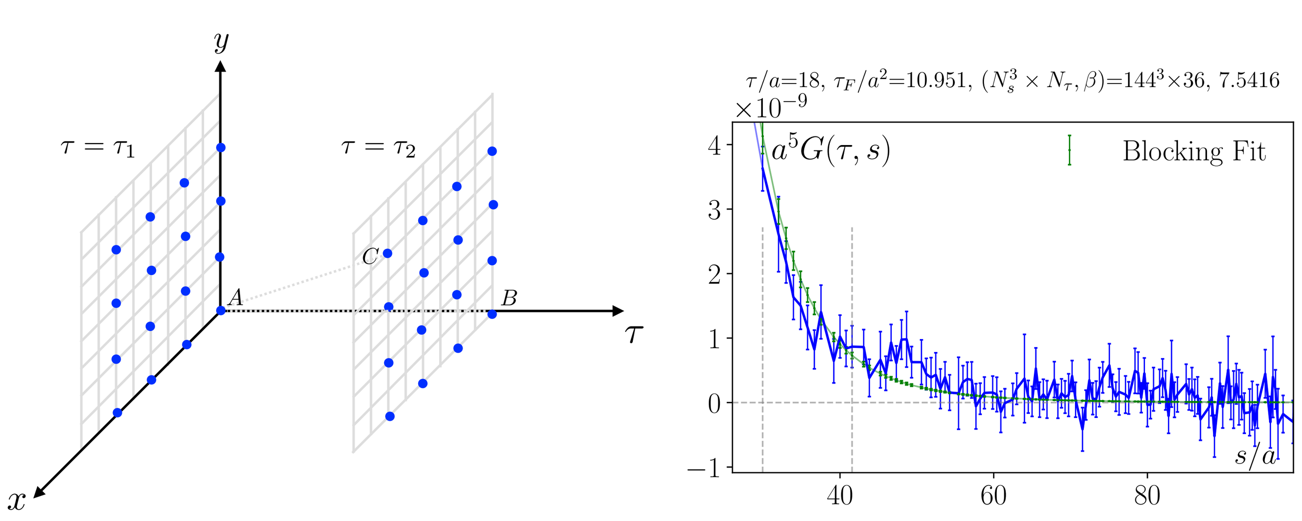

Figure 1. Sketch of blocking method in temporal correlator taken from [6] (left) and the fits of the data (right).

5. Renormalization:

$$T_{\mu\nu}(\tau_F, x) = c_1(\tau_F)\,U_{\mu\nu}(\tau_F, x) + 4c_2(\tau_F)\,\delta_{\mu\nu}E(\tau_F, x).$$

6. Discretization error control: tree level improvement.

$$G^{\text{t.l.}}(\tau T) = G_{\text{lat}}(\tau T)\cdot\frac{G^{\text{LO}}_{\text{cont}}(\tau T)}{G^{\text{LO}}_{\text{lat}}(\tau T)}.$$

7. Data analysis: continuum extrapolation + flow time extrapolation.

Lattice Setup

- **Action:** Wilson gauge action for configuration generation; Symanzik improved action for gradient flow (Zeuthen flow).
- **Temperatures:** $0.76T_c, 0.9T_c, 1.125T_c, 1.267T_c, 1.5T_c, 1.9T_c, 2.25T_c$.
- **Lattices size:**

N_σ	96			120		144	
N_τ	16	24	32	20	30	24	36

β	6.6506	6.7837	6.8268	7.1131	7.1469	7.2989
a (fm)	0.03446	0.02910	0.02757	0.01940	0.01862	0.01552

β	7.0606	7.2005	7.2456	7.3874	7.3986	7.5416
a (fm)	0.02068	0.01746	0.01654	0.01397	0.01379	0.01164

[1] J. E. Bernhard, J. S. Moreland and J. Scott, *Nature Phys.*, 2019, 15(11): 1113-1117.

[2] P. B. Arnold, C. Dogan, and G. D. Moore, *Phys. Rev. D*, 74, 085021 (2006).

[3] N. Astrakhantsev, V. Braguta, and A. Kotov, *JHEP* **04**, 101 (2017).

[4] N. Astrakhantsev, V. Braguta, and A. Kotov, *Phys. Rev. D*, 98, 054515 (2018).

[5] Altenkort L, Eller A M, Francis A, et al, *Physical Review D*, 2023, 108(1): 014503.

[6] L. Altenkort, A. M. Eller, O. Kaczmarek, L. Mazur, G. D. Moore, and H. T. Shu, *Phys. Rev. D*, 105, 094505 (2022).

Analyses

Double Extrapolation: eliminate $\mathcal{O}(a^2)$ discretization effects and recover physical correlators

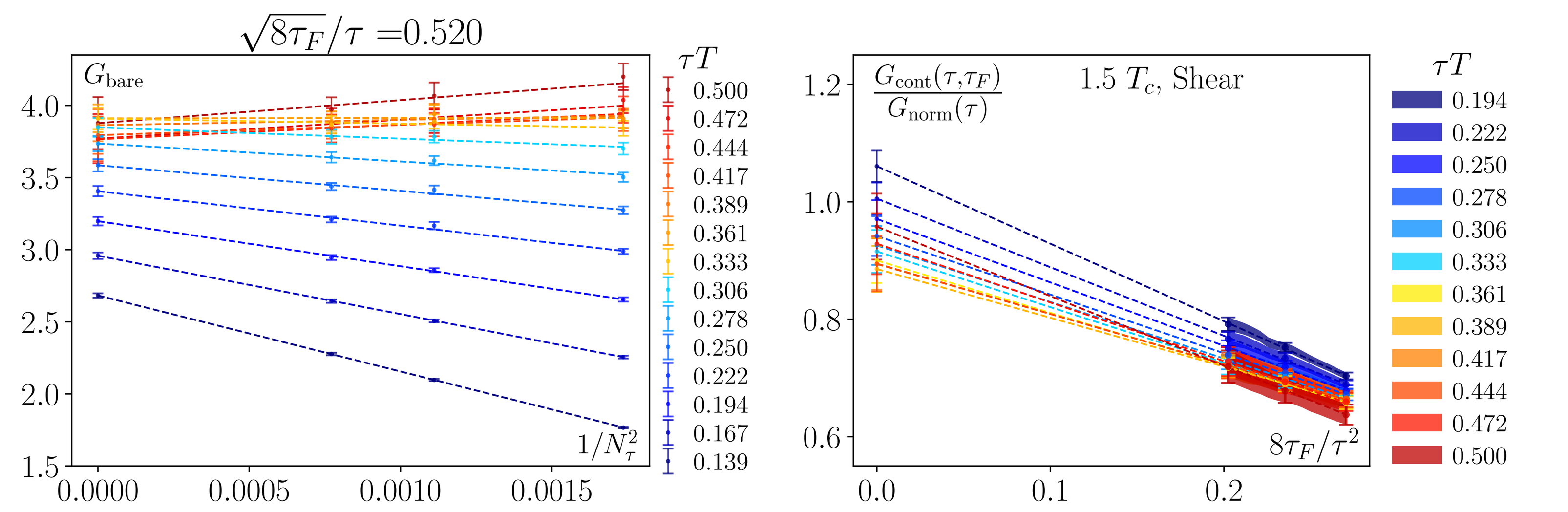

Figure 2. $a \to 0$ extrapolation (left) at 0.9 T_c and $\tau_F \to 0$ extrapolation (right) of the bulk correlators at $1.5T_c$.

Correlators: clear temperature dependencies for both channels

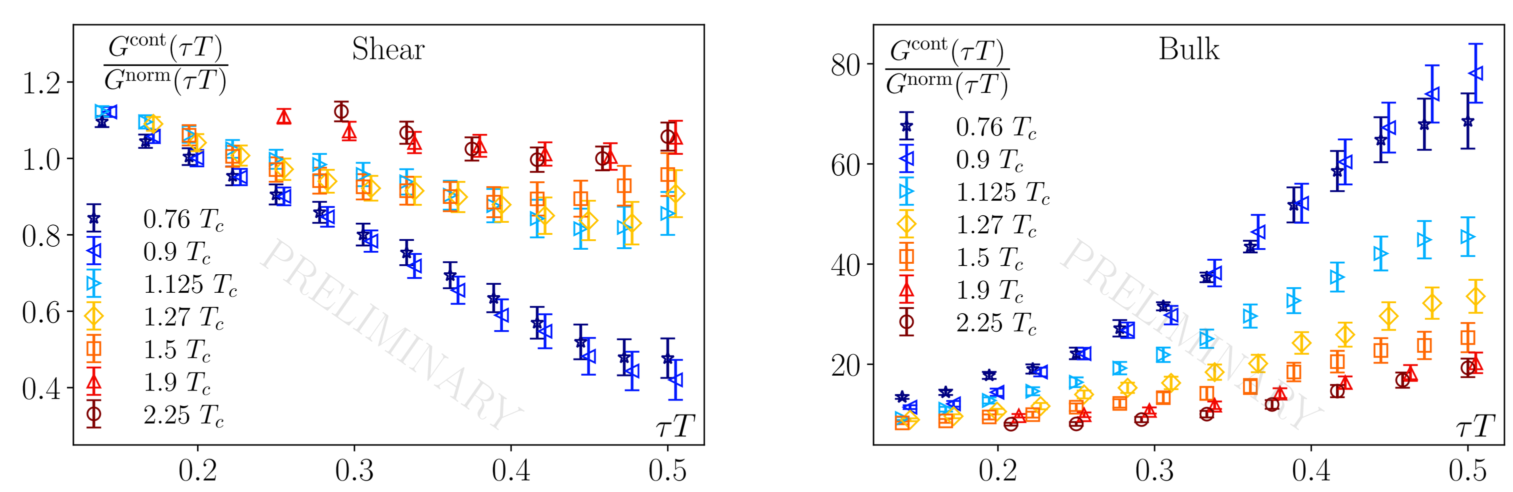

Figure 3. Normalized correlators in the continuum limit.

Spectral Function: model fits

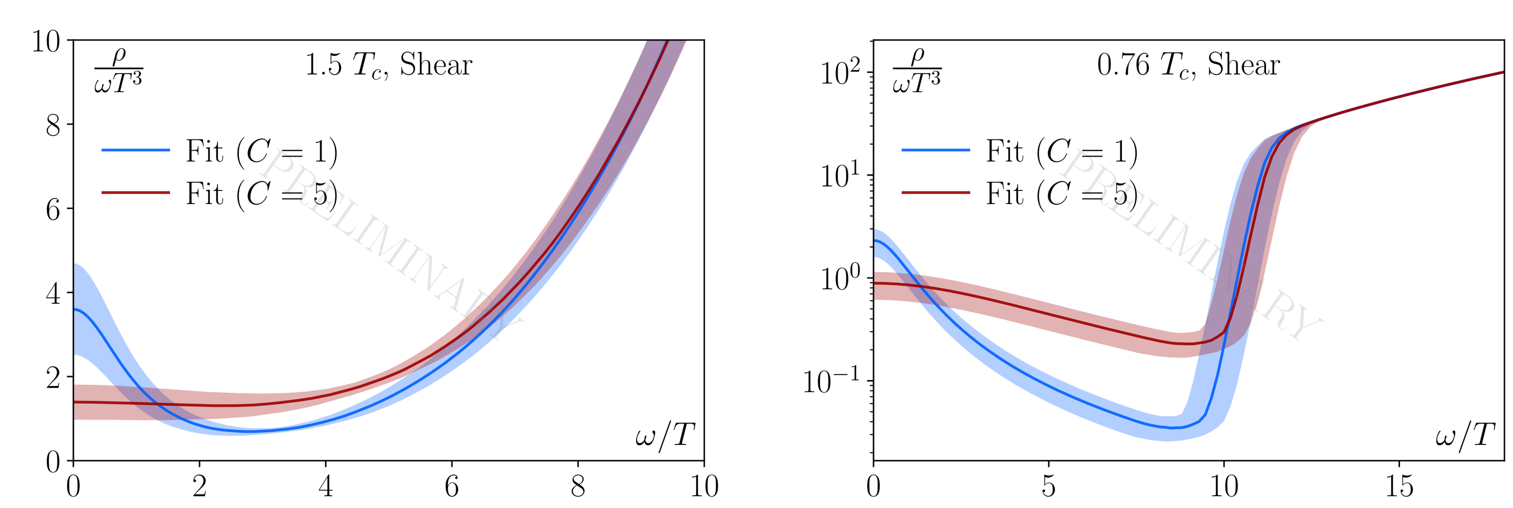

Figure 4. $C = 1$, sharp peak, long-lived excitation; $C = 5$, broad peak, short-lived excitation.

Conclusion

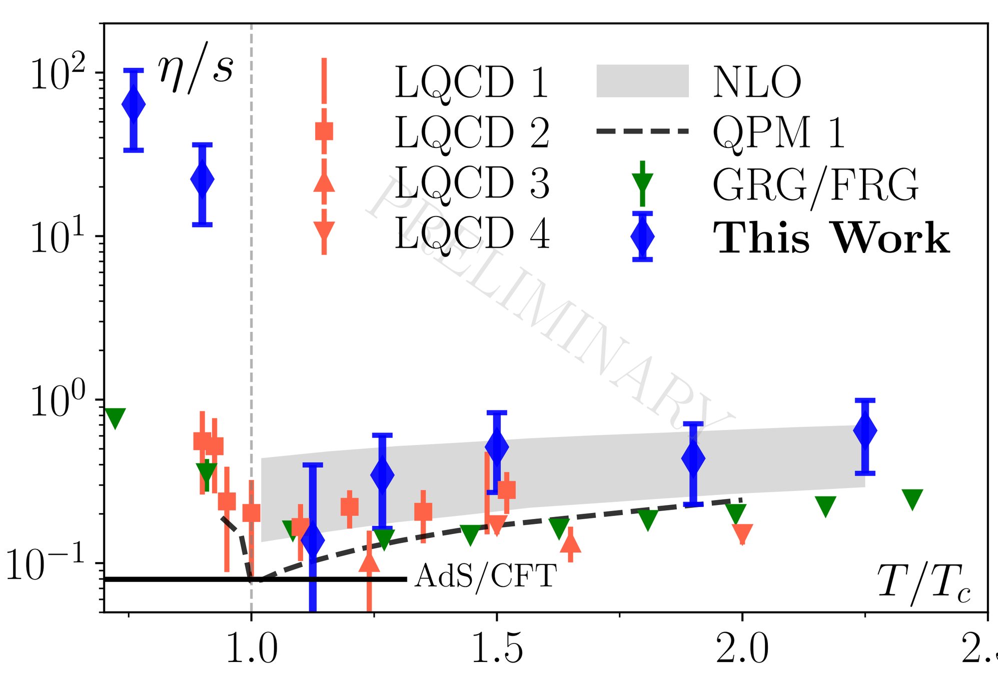

LQCD1: PRD 108, 014503 (2023). GF, $a \geq 0.0117$ fm.
LQCD2: JHEP 04, 101 (2017). ML, $a \geq 0.0253$ fm.
LQCD3: PRD 76, 101701 (2007). ML, $a \geq 0.0476$ fm.
LQCD4: PRD 98, 014512 (2018). ML, $a \geq 0.0157$ fm.
NLO: Ghiglieri et al., JHEP 03, 179 (2018).
QPM 1: Mykhaylova et al., PRD 100, 34002 (2019).
GRG/FRG: Christiansen et al., PRL 115, 112002 (2015).

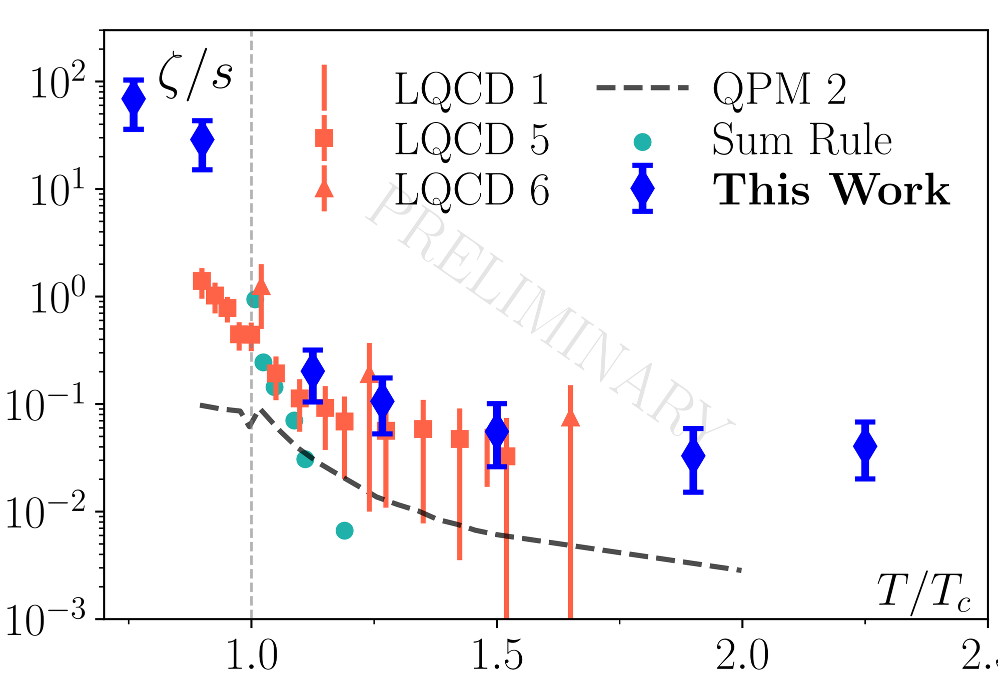

LQCD1: PRD 108, 014503 (2023). GF, $a \geq 0.0117$ fm.
LQCD5: PRD 98, 054515 (2018). ML, $a \geq 0.0253$ fm.
LQCD6: PRL 100, 162001 (2008). ML, $a \geq 0.0317$ fm.
QPM 2: Mykhaylova et al., PRD 103, 014007 (2021).
Sum Rule: Kharzeev et al., JHEP 09, 093 (2008).

- η/s decreases fast at $T < T_c$ but increases mildly with temperature at $T > T_c$.
- For η/s, the "QPM 1", GRG/FRG and "LQCD 2" also predict a similar dip structure.
- η/s approaches the AdS/CFT bound $1/4\pi$ at $T \simeq T_c$.
- $\zeta/s(T < T_c) \gg \zeta/s(T > T_c)$, and ζ/s decreases steadily across the temperature range.
- Sum-rule and other lattice calculations align with the decreasing trend but smaller ζ/s.
- Large and fine lattices with $L_{\max} = 3.3091$ fm and $a_{\min} = 0.01164$ fm are generated.
- Signal quality improved to the $\mathcal{O}(1\%)$ level via gradient flow and blocking method.
- Transport peak + NLO spectral function (the most accurate UV input) describes the data well.
- Systematic uncertainties under control from lattice a and spectral peak width variations.
- Wide temperature range from $0.76T_c$ to $2.25T_c$ of η/s and ζ/s in pure SU(3) gluodynamics.